Available online at www.sciencedirect.com
ScienceDirect
International Journal of Heat and Mass Transfer 50 (2007) 1206–1211
International Journal of HEAT and MASS TRANSFER
www.elsevier.com/locate/ijhmt

Technical Note

Study on the steady-state characteristics of the sensor tube of a thermal mass flow meter

Dong-Kwon Kim, Il Young Han, Sung Jin Kim *

Department of Mechanical Engineering, Korea Advanced Institute of Science and Technology, Taejon 305-701, Republic of Korea

Received 26 January 2006; received in revised form 22 August 2006
Available online 25 October 2006

Abstract

In the present work, a simple numerical model for steady-state heat transfer phenomena occurring in the sensor tube of a thermal mass flow meter (TMFM) is presented. In order to validate the proposed model, extensive experimental investigations are performed. Based on the results from the validated model, a correlation for predicting the linear range of the TMFM is presented. Finally, the effects of engineering parameters on the linear range are investigated.

1. Introduction

The measurement and control of gas flow is critical in many engineering applications, including semiconductor manufacturing processes and chemical processes. Thermal mass flow meters (TMFMs) are most widely used for measuring mass flow rates in the semiconductor industry [1]. A TMFM typically consists of a sensor tube, a bypass (main) tube, and an electric circuit. A sensor tube in a TMFM is a long, slender stainless steel capillary tube with the heating and temperature-sensing wires wrapped around it as shown in Fig. 1(a) [2]. A typical temperature difference between the two temperature sensors is presented in terms of the flow rate in Fig. 1(b). The temperature profile of the sensor tube is symmetric at the zero flow rate. In the linear range, the temperature difference linearly increases with increasing the flow rate. This allows for measurement of the flow rate through the sensing of the temperature difference. However, as the flow rate increases further, the temperature difference attains a maximum value and then decreases with increasing flow rate which causes a TMFM to be no longer useful in measuring the flow rate.

It is obvious that the linear range is one of critical parameters for designing TMFMs. In order to measure various flow rates of gas streams, a TMFM should be applicable to a wide range of the flow rates. The linear range is typically narrower than 10 SCCM unless a bypass tube is used. Therefore, there has been a great deal of attempts to improve the linear range in the industry. However, there has not been a systematic study on the characteristics of the linear range of the TMFM to the authors' knowledge. Even though many research works on the TMFM have been conducted by previous investigators [3–8], they only focused on delineating fluid-flow and heat transfer characteristics of steady-state heat transfer phenomena in the sensor tube. There are no reliable data or correlations by which one can predict the linear range quantitatively.

The present study deals with heat transfer phenomena in a TMFM without a bypass device. In the present work, a simple numerical model for the sensor tube of a TMFM is presented. In order to validate the proposed model, extensive experimental investigations are performed. Based on the results from the validated model, the effects of engineering parameters on the linear range of the TMFM are investigated. Finally, a correlation for predicting the linear range is presented.

* Corresponding author. Tel.: +82 42 869 3043; fax: +82 42 869 8207.
E-mail address: sungjinkim@kaist.ac.kr (S.J. Kim).

0017-9310/$ - see front matter © 2006 Elsevier Ltd. All rights reserved.
doi:10.1016/j.ijheatmasstransfer.2006.08.021

Nomenclature

A	cross-sectional area, m^2
C	heat capacity, J/kg K
D_{in}	inner diameter of the tube, m
D_{out}	outer diameter of the tube, m
L	distance from the center of the sensor tube to the end of the sensor tube, m
L_h	distance from the center of the sensor tube to the end of the heater, m
L_s	distance from the center of the sensor tube to the sensor, m
$\dot{m}$	mass flow rate of the fluid, kg/s
$\Delta\dot{m}_l$	linear range, kg/s
R_r	thermal resistance per unit length for radial heat loss, m K/W
T	temperature, °C
x	axial coordinate

Subscripts

amb	ambient
f	fluid
t	tube

2. Simple numerical model

To analyze heat transfer phenomena in the sensor tube, the physical domain of the sensor tube is divided into two regions. One is a sensor tube region, and the other is an inner fluid region. The energy balance for the each region is represented by

$$k_t A_t \frac{d^2 T_t}{dx^2} + h_i P(T_f - T_t) - \frac{1}{R_r}(T_t - T_{amb}) + q' = 0 \quad (1)$$

$$k_f A_f \frac{d^2 T_f}{dx^2} - \dot{m} C_f \frac{dT_f}{dx} + h_i P(T_t - T_f) = 0 \quad (2)$$

where T_s, T_f, A, h_i, P, R_r, and q' are tube temperature, inner fluid temperature, cross-sectional area, interstitial heat transfer coefficient, wetted perimeter of the tube, thermal resistance per unit length for radial heat loss, and heat flux per unit length supplied from the heater, respectively. The first term on the left-hand side of Eq. (1) is the axial conduction term, and the second term accounts for thermal interaction between the sensor tube and the fluid. The third term denotes a radial heat loss from the outer wall of the tube to the surroundings. Similarly, Eq. (2) consists of the conduction term in the axial direction, the enthalpy change term of the fluid, and the thermal interaction term. Boundary conditions are given as

$$T_t(x = -L) = T_f(x = -L) = T_{amb} \quad (3)$$

$$T_t'(x \to \infty) = T_f'(x \to \infty) = 0 \quad (4)$$

Governing equations are solved by the control-volume-based finite difference method. A power law scheme is used for discretization of the conduction and convection terms. Discretization equations are calculated by the ADI method. All numerical data in the paper are obtained by using the numerical model presented in this section.

3. Experimental validation

An experimental investigation was performed to validate the proposed numerical model. The total experimental apparatus is shown schematically in Fig. 2(a). The nitrogen gas passed through a capillary tube made of stainless steel 304 which had a total length of 91 mm $L = 45.5$ mm. The nitrogen gas was used in the present experiment because typical TMFMs currently employed in semiconductor fabrication processes are calibrated with nitrogen gas. We used capillaries with several inner and outer diameters. The heating wire wound around the tube was made of a nickel–chromium alloy (Ni:80%, Cr:20%), the resistivity of which is independent of the temperature variations. The length of the heater is 14.8 mm. The heater was powered by a DC power supply manufactured by Hewlett–Packard. The sensor housing was connected to a vacuum chamber. This chamber was evacuated by a mechanical pump and an oil diffusion pump in order to eliminate the heat loss due to natural convection from the sensor tube. The gas flowed into the sensor tube from a pressure tank through a metering valve and a solenoid valve. The metering valve was used for setting the volume flow rate. The flow rate of gas was measured by a pre-calibrated TMFM on the downstream side of the sensor tube. This TMFM was Brooks Instrument model 5850. The uncertainty of the TMFM in the range of these experiments was ±1%. We conducted experiments for the flow rate range from 0 to 50 SCCM (standard cubic centimeters per minute). Nine thermocouples were attached to the outer surface of the sensor tube for measuring the wall temperature distributions. The positions of thermocouples for temperature measurement are shown in Fig. 2(b). The measured voltage signals were acquired using a Hewlett–Packard E1326B digital multi-meter and converted into temperatures using Agilent's VEE data acquisition and reduction software. In obtaining the experimental results, we conducted experiments 5 times.

4. Results and discussion

Figs. 3 and 4 show the temperature profiles along the sensor tubes and the temperature differences between the upstream and downstream sensors, respectively. As can be seen from these figures, the results from the simple numerical model are in fair agreement with the experimental

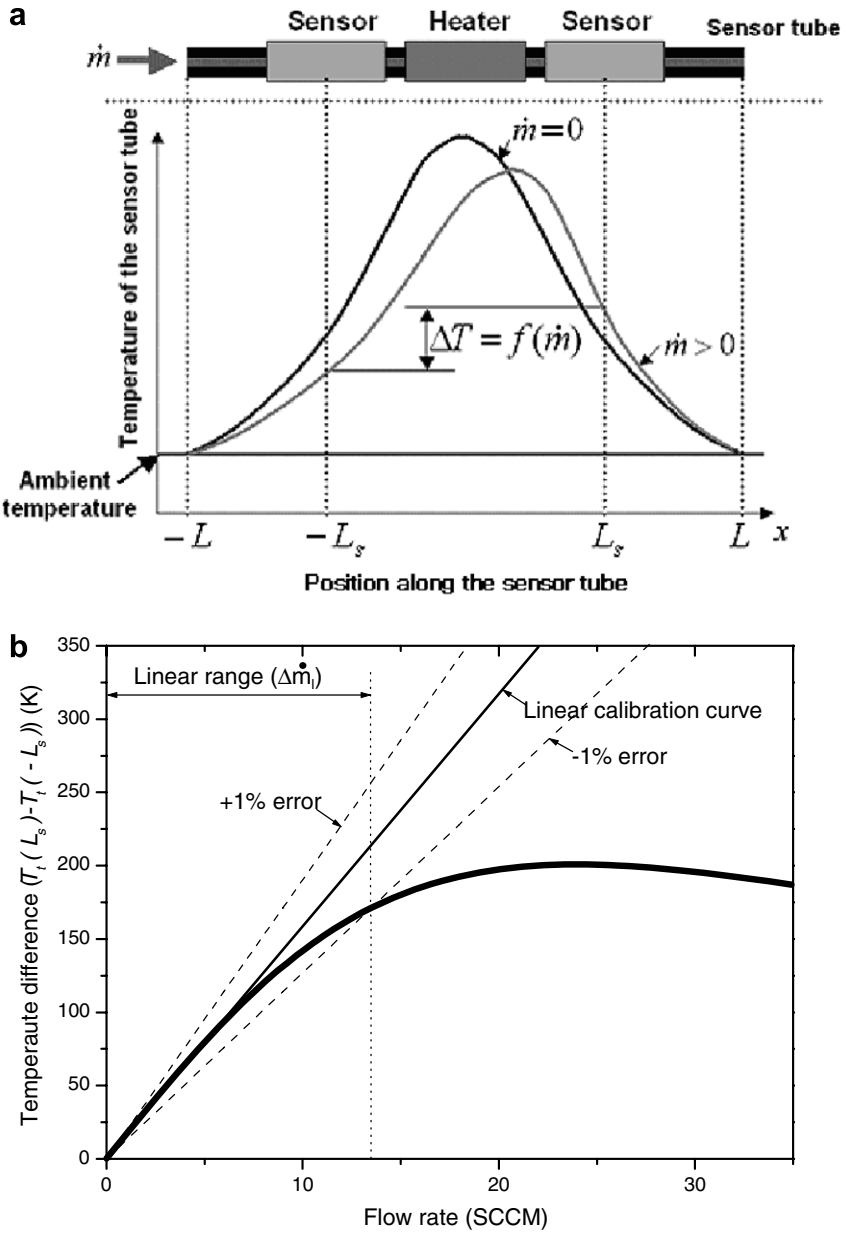

Fig. 1. Measuring principle of the TMFM (a) Schematic layout of the sensor tube and (b) typical output of the TMFM (not in scale).

results. Therefore, the presented model is suitable for predicting the steady-state characteristics of the sensor tube of a TMFM. From Figs. 3 and 4, heat transfer phenomena in the sensor tube can be explained as follows. The temperature difference between the upstream sensor and the downstream sensor is zero at the zero flow, because the temperature profile along the sensor tube is symmetrical. When the gas begins to flow, the incoming cold gas is heated at the upstream section by the tube which is preheated by the heater. When the flow rate is small enough to be in the linear range, the gas temperature increases considerably at the upstream section. In this case, the gas has a higher temperature than the tube when the gas flows into the downstream section. Heat transfers from the gas to the tube along the downstream section as explained in Ref. [6]. Consequently, as the flow rate increases, the upstream tube temperature decreases and the downstream tube temperature increases, which causes the temperature difference to increase. On the contrary, when the flow rate is beyond the linear range, the gas temperature hardly increases due to its large flow rate. In this case, even when the gas flows into the downstream side, the gas still has a lower temperature than the tube. Heat transfer from the tube to the gas still occurs along the downstream section. Accordingly, as the flow rate increases, the upstream and downstream temperatures decrease together and the temperature difference also decreases.

In this paper, the linear range is defined as the range of the flow rate for which a flow meter produces a temperature difference linearly proportional to the flow rate. In

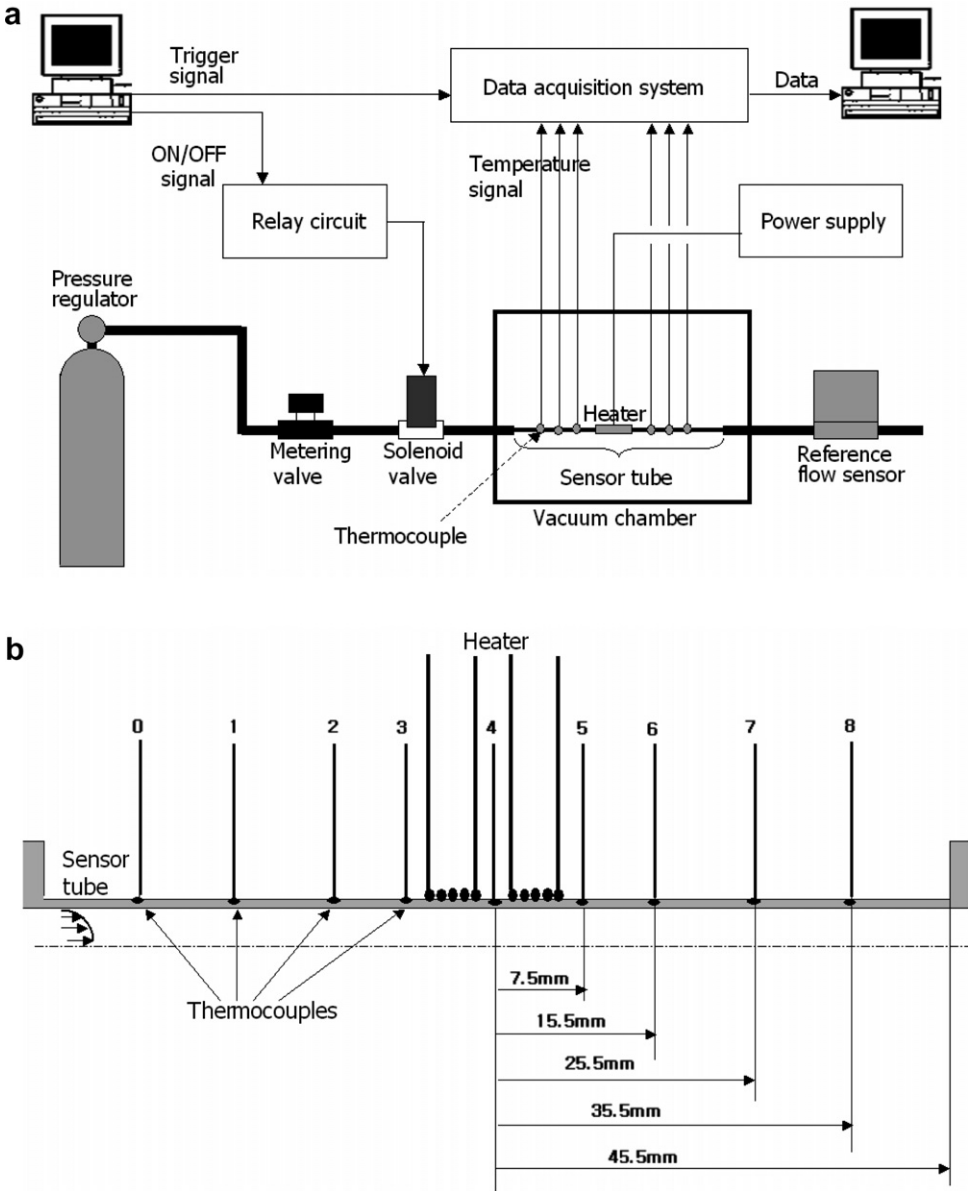

Fig. 2. Experimental apparatus (a) Schematic diagram of the total experimental apparatus and (b) Positions of the heater and thermocouples.

other words, the linear range is given as the follow equation.

$$\frac{1}{\dot{m}}\left(T_t(x=-L_s)-T_t(x=L_s)\right)\Big|_{\dot{m}=\Delta\dot{m}_l} = 0.99\frac{\partial}{\partial\dot{m}}\left(T_t(x=-L_s)-T_t(x=L_s)\right)\Big|_{\dot{m}=0} \quad (5)$$

Based on the numerical results, the correlation for predicting the linear range is obtained. The correlation is given as

$$\frac{\Delta\dot{m}_l C_f L}{k_t A_t} = \left(13.13+25.50\left(\frac{L_s}{L}\right)+36.30\left(\frac{L_s}{L}\right)^2\right)\left(\frac{L^2}{k_t A_t R_r}\right) \times\left(5434-19910\left(\frac{L_s}{L}\right)+18920\left(\frac{L_s}{L}\right)^2+\left(\frac{L^2}{k_t A_t R_r}\right)\right)^{-1} \quad (6)$$

where $\Delta\dot{m}_l C_f L/k_t A_t$ is the dimensionless linear range and $L^2/k_t A_t R_r$ is the dimensionless radial heat loss. The correlation based on the numerical results can be applicable for

$$0.1<\frac{L^2}{k_t A_t R_r}<1000, \quad 0.2<\frac{L_s}{L}<0.6, \quad 0.4<\frac{L_h}{L_s}<0.6 \quad (7)$$

Fig. 5 shows the linear ranges obtained both from the numerical results and from the correlation. The correlation predicts the numerical results within a relative error of 15%. By using the proposed correlation, we investigate the effects of engineering parameters on the linear range:

(1) Heat loss is closely related to the linear range. The linear range increases with increasing heat loss. However the sensitivity decreases with increasing heat loss.

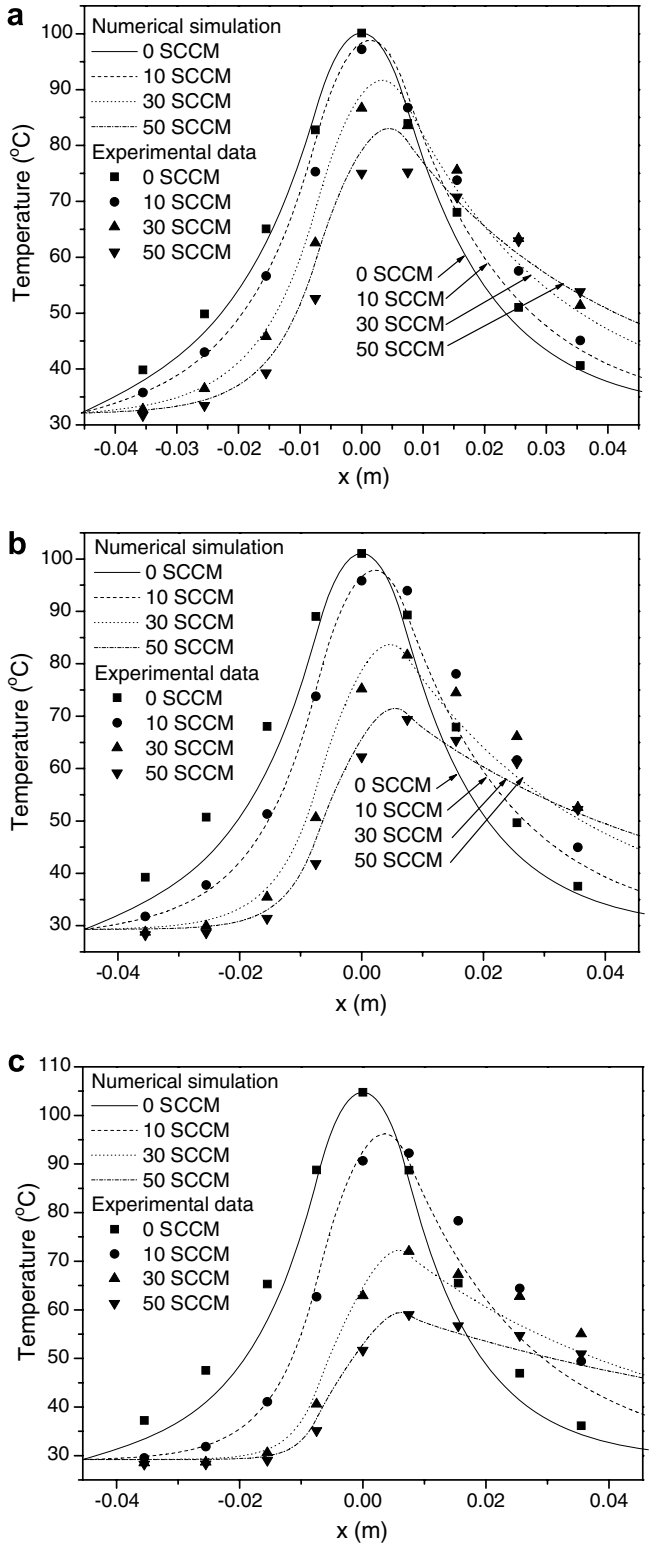

Fig. 3. Tube-wall temperature profiles (a) $D_{out} = 1.257$ mm, $D_{in} = 0.977$ mm, (b) $D_{out} = 0.812$ mm, $D_{in} = 0.562$ mm and (c) $D_{out} = 0.508$ mm, $D_{in} = 0.304$ mm.

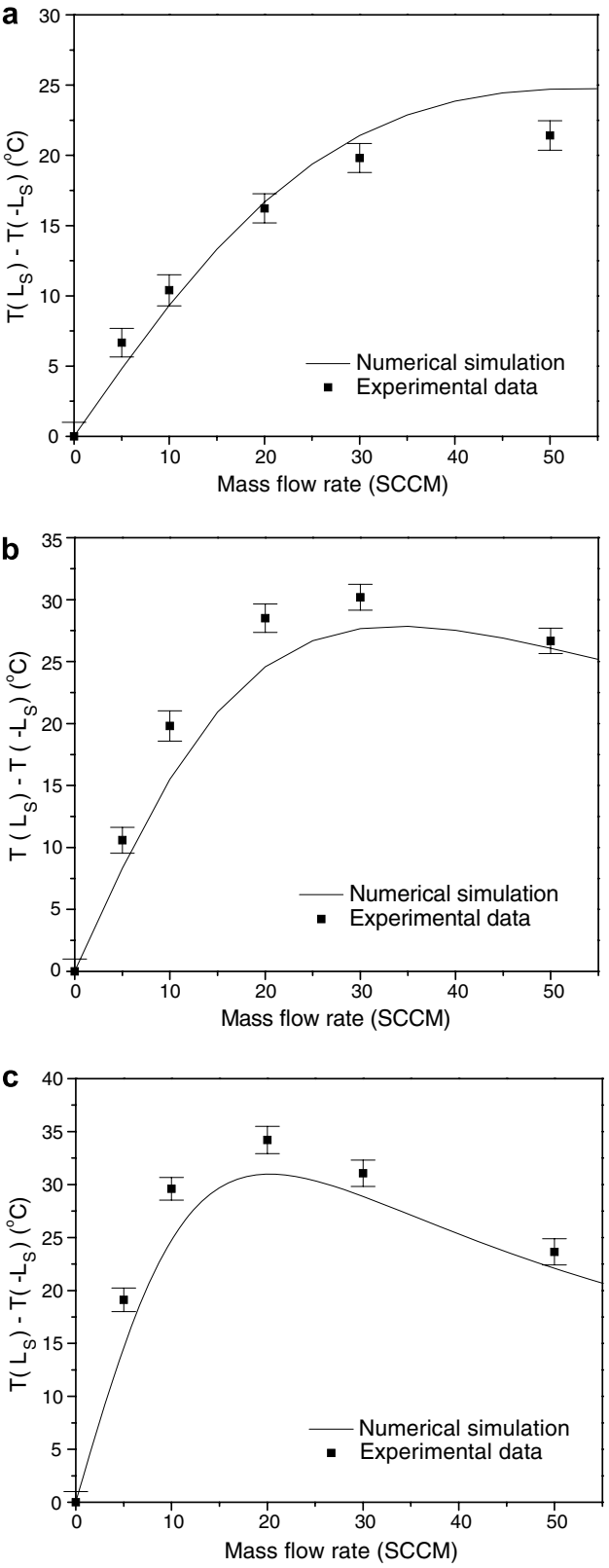

Fig. 4. Temperature differences between two sensors (a) $D_{out} = 1.257$ mm, $D_{in} = 0.977$ mm, $L_s = 7.5$ mm, (b) $D_{out} = 0.812$ mm, $D_{in} = 0.562$ mm, $L_s = 7.5$ mm and (c) $D_{out} = 0.508$ mm, $D_{in} = 0.304$ mm, $L_s = 7.5$ mm.

(2) The linear range increases with increasing tube cross-sectional area. However, the response time also increases with increasing tube cross-sectional area. In addition, the error due to tilting becomes higher.

(3) The linear range increases with decreasing tube length.

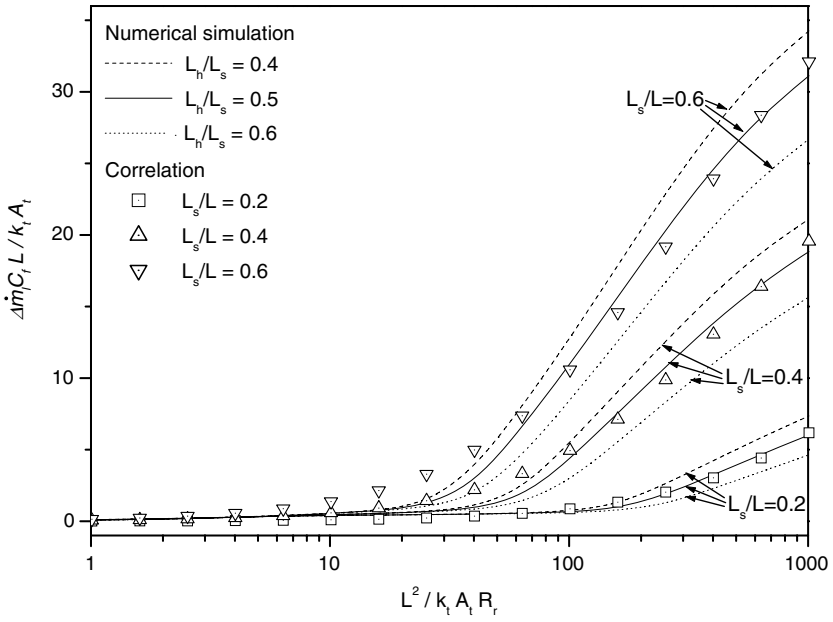

Fig. 5. Comparison between the measurement ranges from the correlation and from the numerical simulation.

(4) When the thermal conductivity of the sensor tube increases, the linear range increases.
(5) When $L^2/k_tA_tR_r < 10$, the linear range does not greatly depend on the sensor position (L_s). But, when $L^2/k_tA_tR_r > 10$, the linear range increases with increasing L_s.
(6) The linear range does not greatly depend on the heater length (L_h) compared to other parameters.
(7) The linear range does not depend strongly on the fluid properties except for the heat capacity.

5. Conclusion

In the present work, a simple numerical model for the sensor tube of a thermal mass flow meter is presented. The proposed model is validated by experimental data. Based on the verified numerical model, a correlation for predicting the linear range of the TMFM is obtained as Eq. (6). The correlation predicts the numerical results within a relative error of 15%. Finally, the effects of engineering parameters on the linear range are investigated.

Acknowledgement

This work was supported by KOSEF (Korea Science and Engineering Foundation) through the National Research Lab Program (Grant No. M1060000022406J000022410).

References

[1] S.A. Tison, A critical evaluation of thermal mass flow meters, J. Vac. Sci. Technol. A 14 (4) (1996) 2582–2591.
[2] P. Rudent, P. Navratil, Design of a new sensor for mass flow controller using thin-film technology based on an analytic thermal model, J. Vac. Sci. Technol. A 16 (6) (1998) 3559–3563.
[3] L.D. Hinkle, C.F. Mariano, Toward understanding the fundamental mechanisms and properties of the thermal mass flow controller, J. Vac. Sci. Technol. A 9 (3) (1991) 2043–2047.
[4] A.E. Widmer, R. Fehlmann, W. Rehwald, A calibration system for calorimeter mass flow device, J. Phys. E: Sci. Instrum. 15 (1992) 213–220.
[5] K. Komiya, F. Higuchi, K. Ohtani, Characteristics of a thermal gas flowmeter, Rev. Sci. Instrum. 59 (3) (1998) 477–479.
[6] S.J. Kim, S.P. Jang, Experimental and numerical analysis of heat transfer phenomena in a sensor tube of a mass flow meter, Int. J. Heat Mass Transfer 44 (2001) 1711–1724.
[7] K. Toda, C. Maeda, I. Sanemasa, K. Ishikawa, N. Kimura, Characteristics of a thermal mass-flow sensor in vacuum systems, Sensors Actuators A 69 (1993) 62–67.
[8] I.Y. Han, D.K. Kim, S.J. Kim, Study on the transient characteristics of the sensor tube of a thermal mass flow meter, Int. J. Heat Mass Transfer 48 (2005) 2583–2592.